Lecture 8 - Integrated Optics in Comms. Systems

Up to now we've looked at various discrete elements of fibre communication systems, including lasers, detectors and fibres. In this lecture I shall be looking at the physics of elements required to pull all these together in an integrated system. These elements include fibre couplers, mixers and splitters, waveguides for integrated optics and elements for multiplexing and de-muliplexing fibres using different wavelength channels. Finally I shall look at the use of solitons, which were introduced in an earlier lecture, in commercial transmission systems.

1 Fibre Connectors, Couplers, Mixers and Splitters

1.1 Fibre Connectors

Although fibres are produced on large drums many kilometres long, when used in a communication circuit they inevitably have to be joined or connected together. This must be done in such a way as to minimize the loss at each connection, otherwise the entire system would become too lossy.

Perhaps the simplest technique for permanently joining fibres together is to use a *fusion splice*. Here (figure 8.1) the fibre ends are held in close proximity and heated up to the material softening point ($\sim 2300\,\mathrm{K}$ in silica). The fibres are then pushed together and the two ends fuse to form a continuous length of fibre. The joint is weak and is usually protected by a resin or epoxy overcoat and a metal cover. Both singe and multimode fibre can be joined in this way, with losses as small as 0.1 dB common.

Sometimes it is impractical to use a fusion splice, where a fibre enters a repeater for example, and a demountable connector is necessary. Unfortunately the use of connectors inevitably introduces losses into the system. These are of two main types: Fresnel losses, caused by back reflection at the silica/air interfaces, and losses associated with misalignment of the end faces. The reflectance of a fibre at normal incidence is:

$$R_{\mathrm{F}} = \left(\frac{n_1 - n_0}{n_1 + n_0}\right)^2$$

where n_0 is the refractive index of the medium between the fibres and n_1 is that of the fibre core. For silica fibre, $n_1 = 1.48$ so we have:

$$R_{\mathrm{F}} = \left(\frac{1.48 - 1}{1.48 + 1}\right)^2 = 0.0375.$$

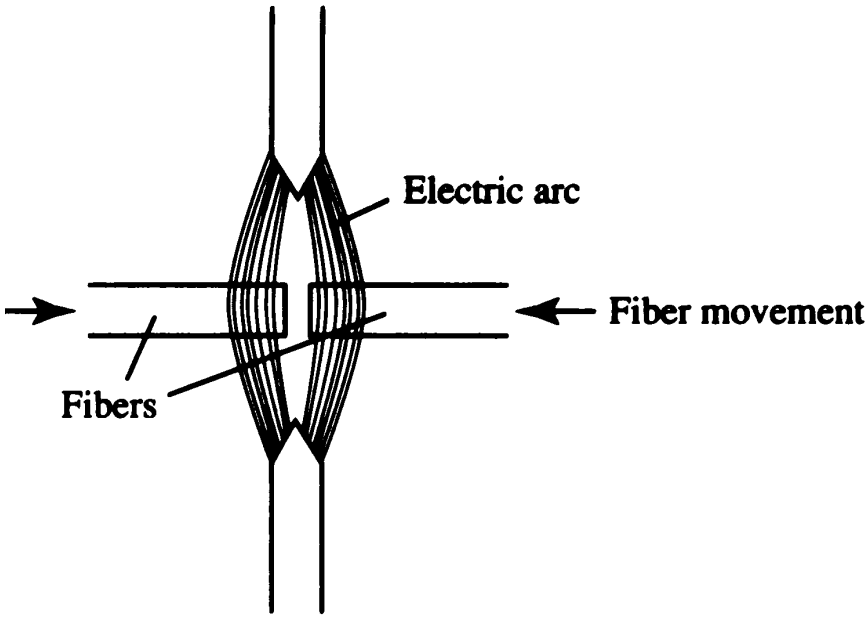

Figure 8.1 In fusion splicing, the fibre ends are pushed together whilst being heated within an electric arc.

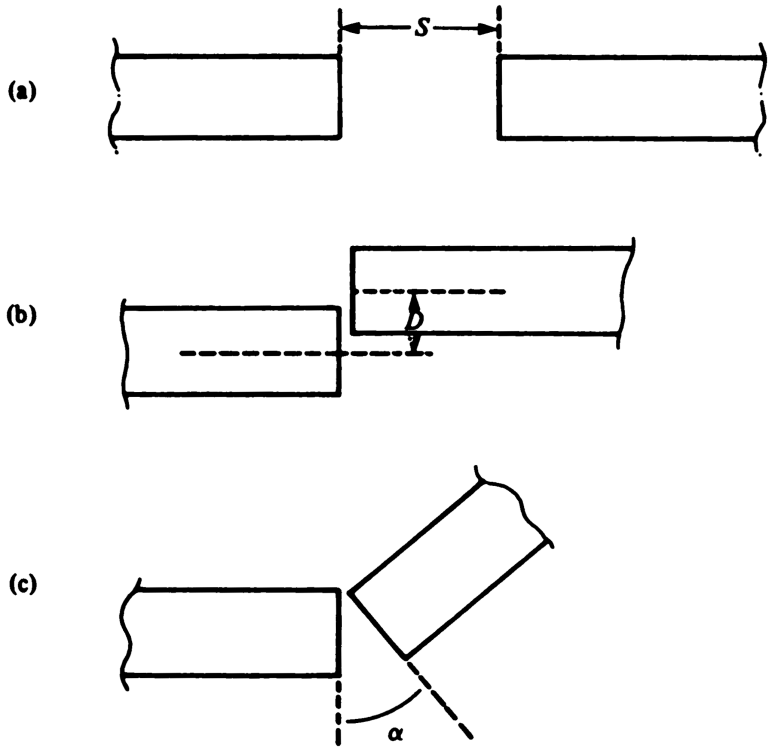

Figure 8.2 Illustration of the three types of misalignment mentioned in the text: (a) longitudinal; (b) lateral and (c) angular misalignment. The parameters used to describe these (S, D and α) are also shown.

Thus the transmission is $1-0.0375 = 0.9625$. This corresponds to a loss of $-10\log(0.9625) = 0.17\,\mathrm{dB}$.

The second type of loss associated with butt-type connections arises from misalignment between the fibres. There are three basic type to be considered: (a) the distance between the fibres along the fibre axis (longitudinal); (b) the offset distance perpendicular to the fibre axis (lateral); and (c) the angle between the two axes of the fibres (angular). These are illustrated in figure 8.2. Lateral loss is the most significant, the transmission losses resulting from lateral misalignment can be written:

$$T_{\mathrm{lat}} = \frac{2}{\pi}\left\{\cos^{-1}\left(\frac{D}{2a}\right) - \frac{D}{2a}\left[1-\left(\frac{D}{2a}\right)^2\right]^{1/2}\right\}$$

where D is the lateral displacement and a the fibre core radius. As an example consider a multimode step index fibre with a lateral misalignment of 10% of the fibre diameter. Thus $D/2a = 0.1$. The transmission becomes:

$$T_{\mathrm{lat}} = \frac{2}{\pi}\left\{\cos^{-1}(0.1) - 0.1[1-(0.1)^2]^{1/2}\right\} = 0.873$$

and the transmission loss is therefore $-10\log(0.873) = 0.59\,\mathrm{dB}$. If Fresnel losses from the example above were also added, the total loss would be $0.17 + 0.59 = 0.76\,\mathrm{dB}$. A typical connector used in commercial systems is illustrated in figure 8.3. In general single mode fibres are much more sensitive to coupling losses than their multimode counterparts, as might be expected from the small core size.

1.2 Fibre Couplers

In a fibre optic communication system it is advantageous to be able to shift power around between fibres without having to go to the expense of coming out of the fibre into an electronic device, performing the desired manipulation, and then re-transmitting the modified signal along the fibre. Furthermore, in an ideal system, in-line fibre-optic components are needed to perform various other functions such as modulation, filtering, polarizing etc. The various kinds of fibre-optic components can be broadly classified as follows:

1. Amplitude/intensity components

   Couplers, Splitters, Amplifiers, Attenuators, Reflectors

2. Phase components

   Phase shifters, Phase modualtors

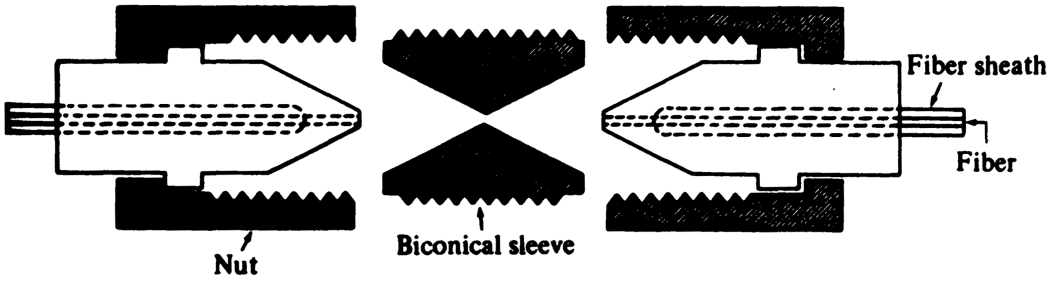

Figure 8.3 (a) Schematic diagram of a biconical demountable connector for but joining optical fibres.

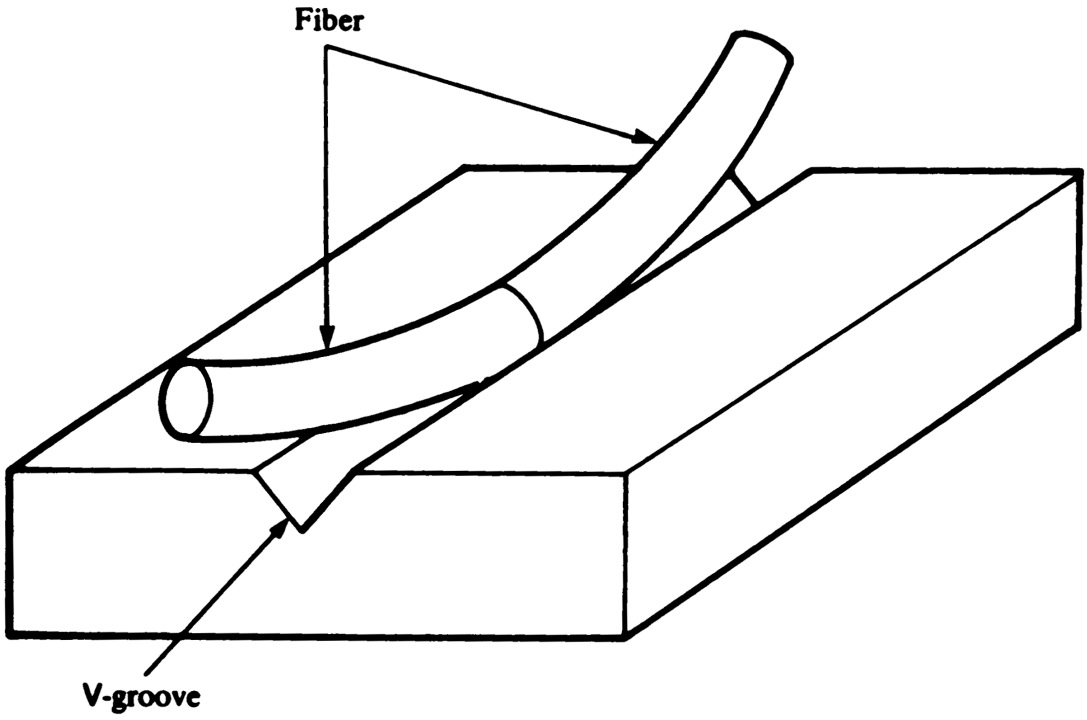

Figure 8.3 (b) Illustration of the use of a V-groove for the alignment of fibre ends prior to joining.

3. Polarization components

   Polarizers, Polarization splitters, Polarization controllers

4. Wavelength components

   Wavelength filters, Wavelength division multiplexers/demultiplexers

5. Frequency components

   Frequency shifters, Filters

6. Active components

   Fibre amplifiers

In this part of the lecture I will look at the principles behind the operation of some of the above devices. A fuller description can be found in *Introduction to Fiber Optics* by A. Ghatak and K. Thyagarajan.

1.3 The Optical Fibre Directional Coupler

The optical fibre directional coupler is the guided wave equivalent of a bulk optic beam splitter and is one of the most important in-line fibre components. It is based on the fact that the modal field of the guided mode extends far beyond the core-cladding interface. Thus when two fibre cores are brought sufficiently close to each other laterally, so that their modal fields overlap, then the modes of the two fibres become coupled and power can transfer periodically between the two fibres. If the propagation constants of the modes of the individual fibres are equal, then this power exchange is complete. On the other hand, if their propagation constants are different, then there is still a periodic, but incomplete, exchange of power between the fibres.

Directional couplers have many interesting applications in power splitting, wavelength division multiplexing/demultiplexing, polarization splitting, fibre optic sensing and so forth.

Consider a directional coupler formed of two, in general, nonidentical single-mode fibres supporting the LP_{01} modes with propagation constants β_1 and β_2. It can be shown (after much algebra!) that if $P_1(0)$ is the power launched into fibre 1 at $z = 0$, then at any value of z the powers propagating in the two fibres are:

$$\frac{P_1(z)}{P_1(0)} = 1 - \frac{\kappa^2}{\gamma^2} \sin^2 \gamma z$$

$$\frac{P_2(z)}{P_1(0)} = \frac{\kappa^2}{\gamma^2}\sin^2\gamma z$$

where

$$\gamma^2 = \kappa^2 + \frac{1}{4}(\Delta\beta)^2$$

and

$$\Delta\beta = \beta_1 - \beta_2$$

In the above equations κ is called the coupling coefficient and is a measure of the strength of the interaction between the two fibres, which depends on the fibre parameters, the separation of the cores and the wavelength of operation. The parameter β is referred to as the *phase mismatch*. Note that, from above,

$$P_1(z) + P_2(z) = P_1(0)$$

independent of z. This is nothing but a statement of conservation of power.

If the two fibres are separated by a distance which is large compared with the mode size then there is now interaction between them. In this case $\kappa = 0$ and we have

$$P_1(z) = P_1(0) \quad P_2(z) = 0$$

Now consider the two cases of phase matching and non-phase matching.

1.3.1 Phase matched case

Assume that the fibres are identical. Then if $\Delta\beta = 0$ we get

$$\begin{aligned} P_1(z) &= P_1(0)\cos^2\kappa z \\ P_2(z) &= P_1(0)\sin^2\kappa z \end{aligned}$$

Figure 8.4 shows the variation of the powers in the two fibres as a function of z. There is a periodic exchange of power between the two fibres, and when

$$z = 0, \frac{\pi}{\kappa}, \frac{2\pi}{\kappa}, \ldots = \frac{m\pi}{\kappa}; \quad m = 0, 1, 2, \ldots$$

$P_1(z) = P_1(0)$ and $P_2(z) = 0$ — that is, the entire power is in the input fibre. When

$$\begin{aligned} z &= \frac{\pi}{2\kappa}, \frac{3\pi}{2\kappa}, \frac{5\pi}{2\kappa}, \ldots \\ &= \left(m + \frac{1}{2}\right)\frac{\pi}{\kappa}; \quad m = 0, 1, 2, \ldots \end{aligned}$$

$P_1(z) = 0$ and $P_2(z) = P_1(0)$ and the entire power is in the other fibre. The minimum distance at which the power completely transfers from the input fibre to the other fibre is given by

$$z = L_c = \frac{\pi}{2\kappa}$$

and is referred to as the coupling length. Strong interaction implies a large value of κ and, hence, a small coupling length.

For typical single-mode fibres operating at a wavelength of 1.3 μm, $\kappa \sim 0.8\,\mathrm{mm}^{-1}$ to $0.3\,\mathrm{mm}^{-1}$, leading to a coupling length of $\sim 2 - 5\,\mathrm{mm}$.

1.3.2 Non-phase matched case

Here $\beta_1 \neq \beta_2$. The equations governing the relative power in each fibre do not simplify in this case so we'll look at some specific values of $\Delta\beta/2\kappa$. The variation of $P_2(z)$ for $\Delta\beta/2\kappa = 0.1, 1$ and 5 are plotted in figure 8.5. From the figure we note that:

- If $\Delta\beta \neq 0$, there is an incomplete transfer of power. In fact the maximum fractional power that is transferred from the input fibre to the coupled fibre is given by

$$\begin{aligned} \eta_{\max} &= \frac{P_{2,\max}}{P_1(0)} = \left(\frac{\kappa^2}{\gamma^2}\,\sin^2\gamma z\right)_{\max} \\ &= \frac{\kappa^2}{\gamma^2} = \frac{1}{1 + (\Delta\beta/2\kappa)} \end{aligned}$$

  Thus, for complete power exchange, we must have $\Delta\beta = 0$; the larger the ratio $\Delta\beta/2\kappa$ the smaller is the fractional power transfer. For example, for $\Delta\beta/2\kappa = 0.1, 1$ and 5, the maximum fractional power transferred is 0.99, 0.5 and 0.04. Hence very little transfer of power will take place between two highly non-phase-matched fibres, even if their cores lie close to each other as long as $\Delta\beta/2\kappa \gg 1$.

- Note also from figure 8.5 that for larger $\Delta\beta/2\kappa$ values, the oscillations in power become more and more rapid in z. This effect is used in integrated optics for realizing optical switches, in wavelength multiplexers/demultiplexers, in polarization splitting using birefringent fibres and so on.

Figure 8.6(a) shows a three dimensional plot of variation in the transverse intensity pattern along the propagation direction for a pair of identical planar waveguides. The corresponding density plot clearly showing complete power transfer is shown in figure 8.6(b). Figures 8.7(a) and (b) show the corresponding plots for a pair of non-identical planar waveguides.

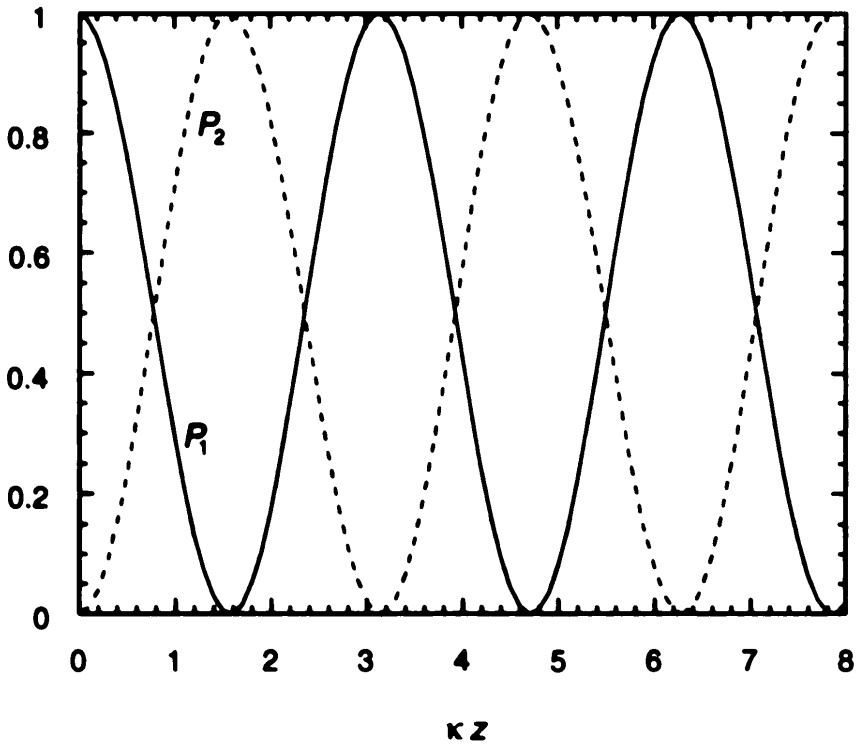

Figure 8.4 Variation of powers in the two fibres in a directional coupler as a function of z when the two fibres have the same propagation constant.

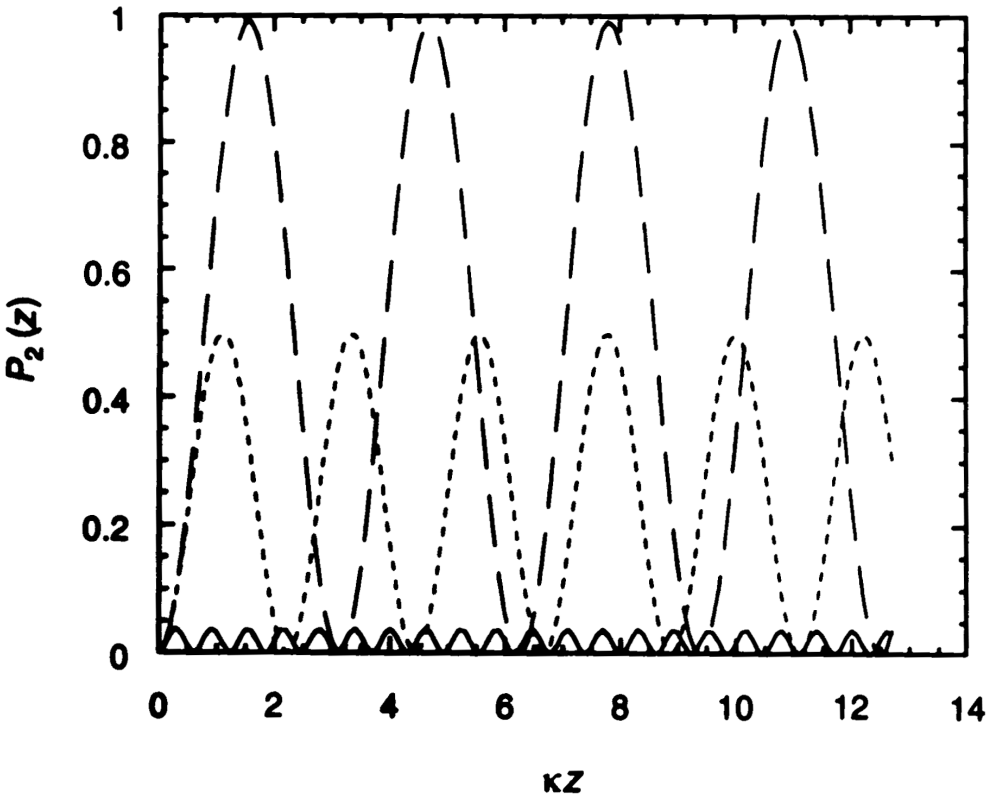

Figure 8.5 Variation of power in the coupled fibre plotted as a function of κz for different values of relative phase mismatch $\Delta\beta/2\kappa$. For $\Delta\beta \neq 0$, the power transfer is always incomplete. The larger the value of $\Delta\beta/2\kappa$, the smaller is the fractional power transfer. The three curves correspond to $\Delta\beta/2\kappa = 0.1$ (long dash), 1.0 (small dash) and 5.0 (solid).

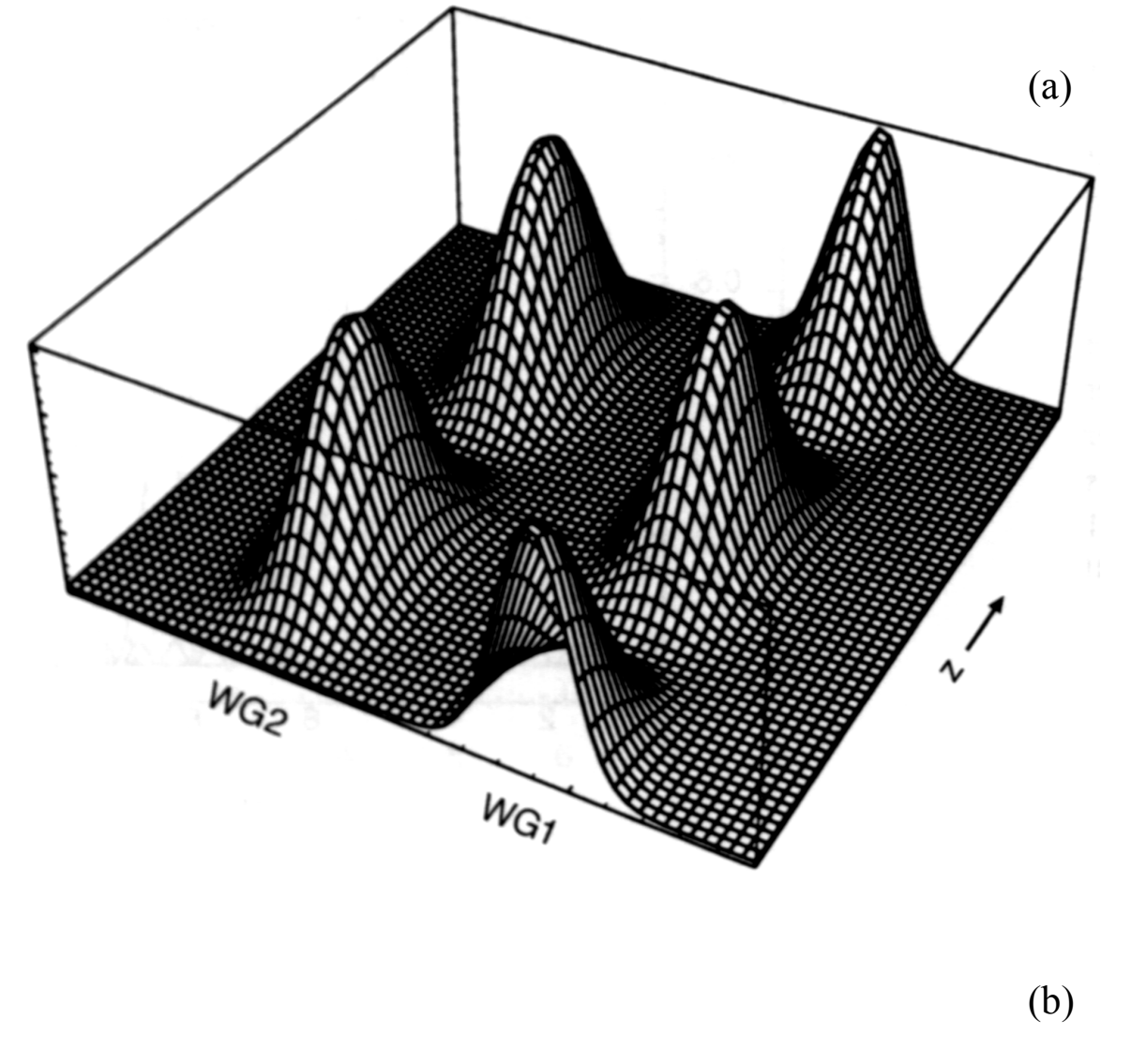

Figure 8.6 (a) Three-dimensional plot of variation of power with propagation length in a directional coupler with $\Delta\beta = 0$. Note that the power exchange between the two waveguides (WG1 and WG2) is complete. (b) The corresponding density plot.

1.3.3 Practical parameters of a coupler

If power P_i is launched into the input port of a directional coupler as shown in figure 8.8 and if the transmitted power, coupled power and back-coupled power are $P_t, P_c,$ and P_r, respectively, then the various characteristics of the coupler are:

$$\begin{aligned}
\text{Coupling ratio } R(\%) &= \frac{P_c}{P_c + P_t} \times 100 \\
R(\text{dB}) &= 10 \log \left[\frac{P_t + P_c}{P_c} \right] \\
\text{Excess loss } L_i(\text{dB}) &= 10 \log \left[\frac{P_i}{P_t + P_c} \right] \\
\text{Insertion loss} &= 10 \log \left[\frac{P_i}{P_c} \right] \\
&= \text{Coupling ratio } + \text{ excess loss} \\
\text{Directivity } D(\text{dB}) &= 10 \log \left[\frac{P_r}{P_i} \right]
\end{aligned}$$

Good directional couplers have low insertion loss and high directivity. Commercially available directional couplers have coupling ratios from 50/50 to 1/99, excess loss $\leq 3.4\,\text{dB}$ (for 3-dB coupler), and directivity of better than $-55\,\text{dB}$.

1.3.4 Fabrication of fibre directional couplers

To fabricate a directional coupler the cladding has to be thinned so as to bring the cores into close proximity. Two main techniques have been developed to accomplish this.

1. Polished fibre couplers.

   Polished fibre couplers rely on exposing the core of the fibre by mechanically polishing off the cladding along one side of the fibre. This is achieved by first bonding the fibre to a curved groove cut in a fused silica block. The whole assembly is then polished to nearly expose the core. This is illustrated in figure 8.9.

   A directional coupler is formed by mating two such polished fibre blocks (see figure 8.10). Usually the space between the substrates is filled with index matching fluid.

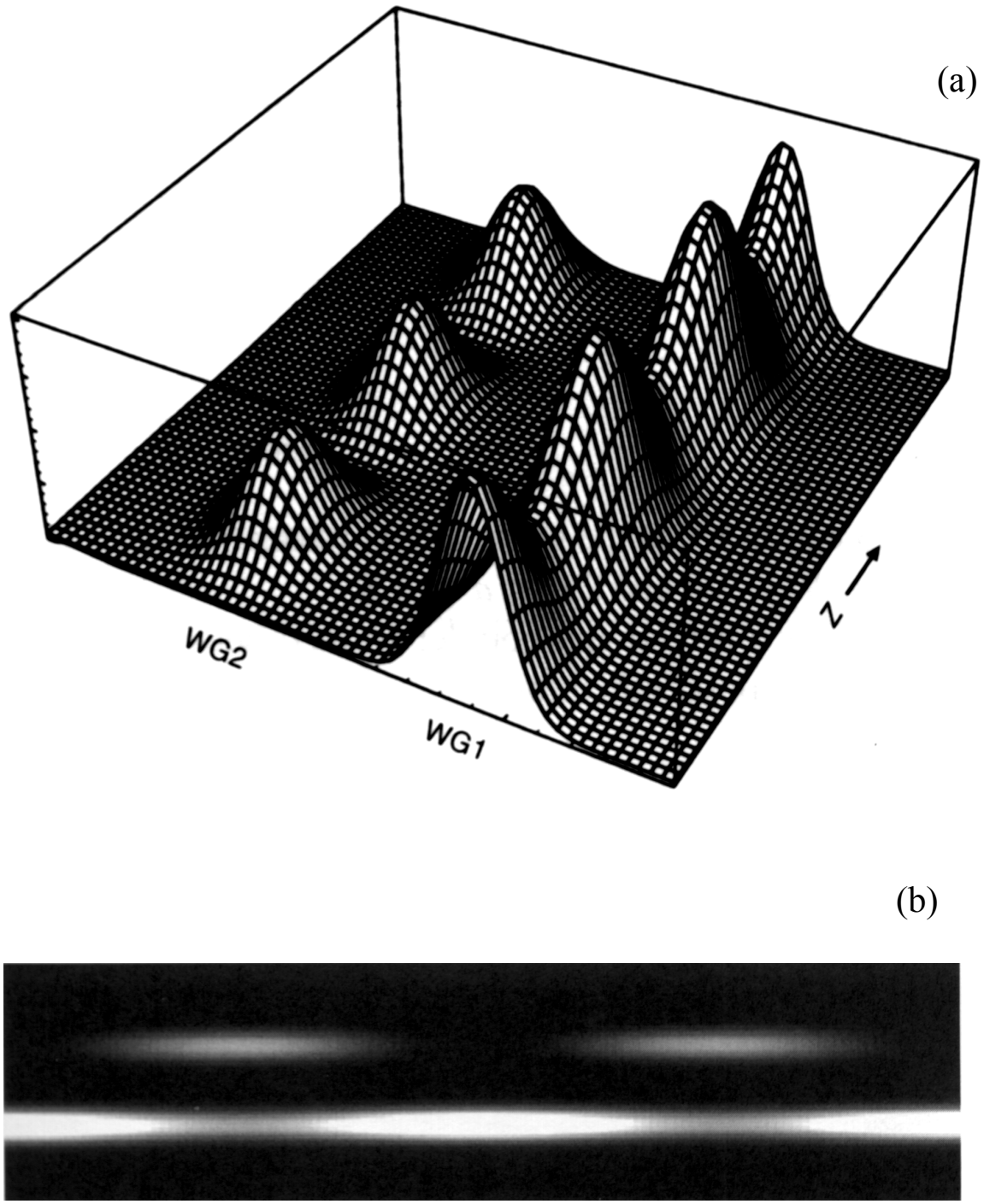

Figure 8.7 (a) Three-dimensional plot of variation of power with propagation length in a directional coupler with $\Delta\beta \neq 0$. Note that the incomplete transfer between the two waveguides (WG1 and WG2) is complete. (b) The corresponding density plot.

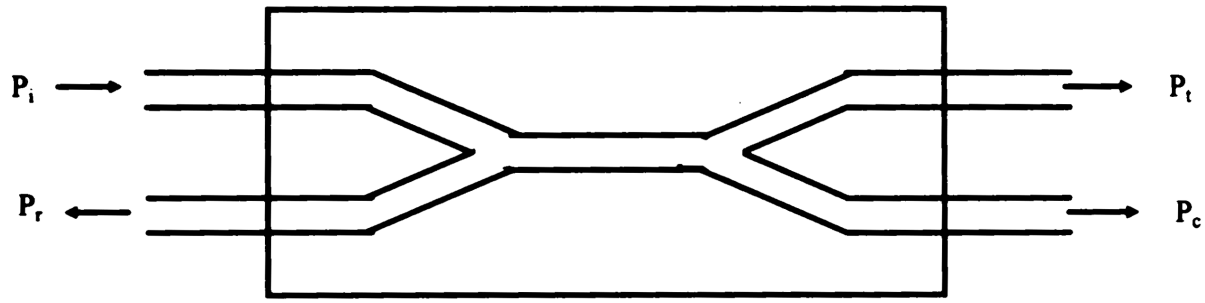

Figure 8.8 For an input power P_i, the transmitted power, coupled power and back-coupled power are P_t, P_c and P_r. An ideal directional coupler would have $P_r = 0$ and $P_t + P_c = P_i$.

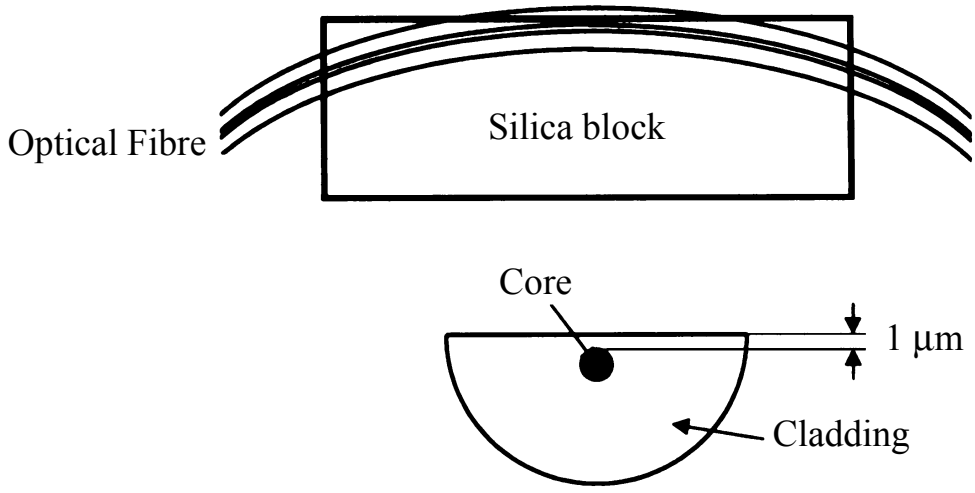

Figure 8.9 A polished fibre half block fabricated by side polishing the cladding.

One of the principal advantages of a polished fibre directional coupler is tunability (figure 8.11). By moving one block laterally with respect to the other (figure 8.10), it is possible to change the core separation. This in turn changes κ and, hence, the power coupled. Such couplers are sometimes referred to as tunable directional couplers.

The directivity of polished couplers is usually excellent, values as small as $-70\,\mathrm{dB}$ have been realised. The insertion loss is also low ($\sim 0.01\,\mathrm{dB}$).

2. Fused couplers.

   Although polished fibre couplers have excellent characteristics, fabricating them is a time-consuming operation. In contrast, fused directional couplers are easier to fabricate and their fabrication can be automated without much difficulty. Fused couplers are fabricated by first slightly twisting two single-mode fires (after removing their protective coating) and then heating them so that the fibres fuse laterally with one another and are also tapered (figure 8.12). Figure 8.13 shows the cross-section of a fused fibre coupler composed of polarization preserving fibres. The two cores lie close to each other. The coupling ratio is monitored on-line as the fibres are fused and drawn. The directivity can be $\sim -55\,\mathrm{dB}$, with losses of $< 0.1\,\mathrm{dB}$.

1.4 Applications

1.4.1 Power dividers

As I mentioned earlier, one of the most important applications of fibre directional couplers is as power dividers. In many applications, such as local area networks or in fibre optic sensing, it is necessary to split or combine optical beams. A fibre directional coupler forms an ideal component since it is compact, cheap and possesses low loss.

1.4.2 Wavelength division multiplexers/demultiplexers

A second very important application of such couplers is in wavelength division multiplexing /demultiplexing. Fibre directional couplers are wavelength sensitive in general, since the propagation constant of the modes and the coupling coefficient κ are functions of wavelength. As an example, consider a directional coupler of length L made of identical fibres and let κ_1 and κ_2 be the coupling coefficients at wavelengths λ_1 and λ_2 so that

$$\kappa_1 L = m\pi$$

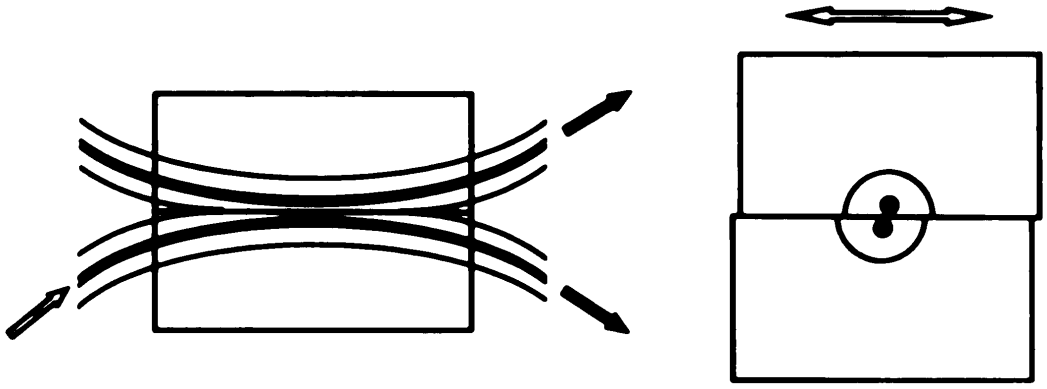

Figure 8.10 A fibre directional coupler made up of two side-polished fibre half blocks. Tuning is achieved by moving one block against the other.

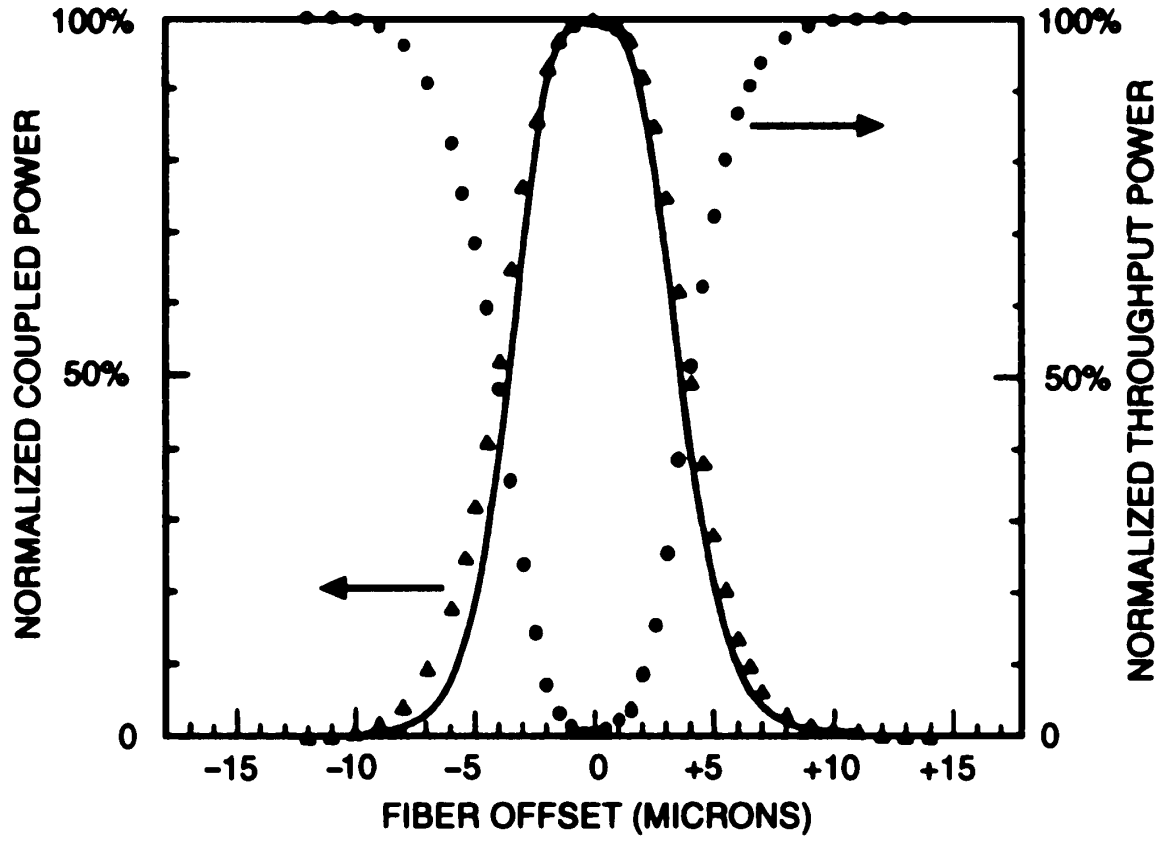

Figure 8.11 Experimental points and theoretical curve (solid line) showing the tunability of a side-polished fibre directional coupler. The figure corresponds to a wavelength of 633 nm.

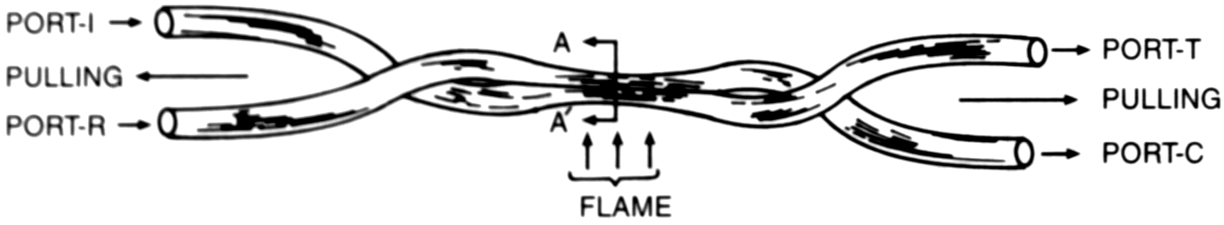

Figure 8.12 Schematic experimental setup for the fabrication of fused fibre directional couplers. The outputs at ports T and C are used for on-line control of the fabrication process.

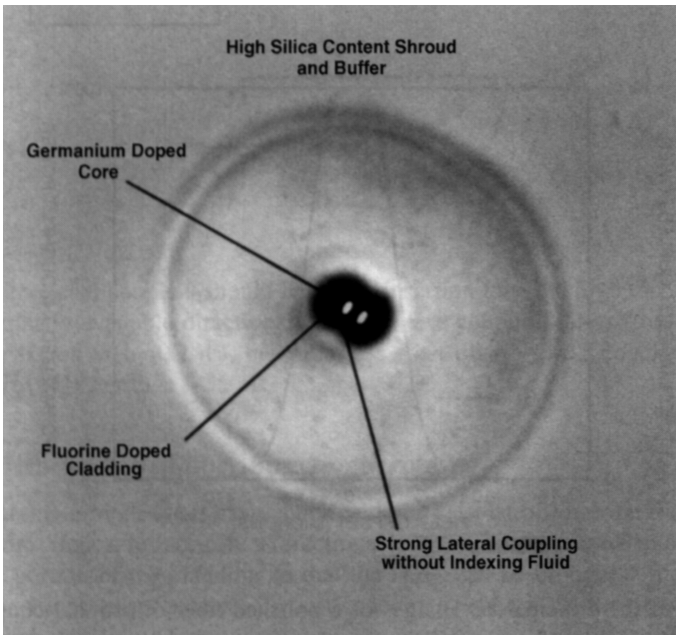

Figure 8.13 The cross section in the fused region of a fused fibre coupler composed of two polarization-preserving fibres. Note the proximity of the two cores.

and

$$\kappa_2 L = \left(m - \frac{1}{2}\right)\pi.$$

In such a case, if light beams at λ_1 and λ_2 are launched simultaneously into the input fibre, then for light at λ_1

$$P_2(\lambda_1, L) = P_1 \sin^2(\kappa_1 L) = 0$$

and for light at λ_2

$$P_2(\lambda_2, L) = P_1 \sin^2(\kappa_2 L) = P_i$$

Thus, light at λ_1 will exit from the input fibre and that at λ_2 will exit from the other fibre (as illustrated in figure 8.14). Such a device forms a wavelength demultiplexer. The same device can also operate as a wavelength multiplexer.

As an example, consider a demultiplexing coupler made of identical fibres with the following specifications: $n_1 = 1.4525,\ n_2 = 1.45$ and $a = 5.6\,\mu$m. We have also that

$$\kappa_1 = \kappa(1.55\,\mu\text{m}) = 6.496\,\text{cm}^{-1}$$

and

$$\kappa_2 = \kappa(1.30\,\mu\text{m}) = 4.872\,\text{cm}^{-1}$$

(note that $\kappa_1 > \kappa_2$ due to greater field penetration in the cladding of the field at $1.55\,\mu$m compared with $1.3\,\mu$m). For an interaction length of 9.67 mm, we have

$$\kappa_1 L \simeq 2\pi \quad \text{and} \quad \kappa_2 \text{L} \simeq \frac{3}{2}\pi.$$

Since the coupling length is given by $\pi/2\kappa$, the coupler has four coupling lengths at $1.55\,\mu$m and three coupling lengths at $1.3\,\mu$m, as illustrated in figure 8.14 (b). Thus the device splits the two-colour beam into its constituent parts.

2 Integrated Optics

2.1 Introduction

Although signal transmission using light waves is now well established, the optical signal usually has to be converted back into an electrical one if any processing needs to be done. The aim of integrated optics (IO) is to be able to carry out as much signal processing as possible on the optical signal itself. Thus optical and electro-optical elements in thin film planar form are used, allowing the assembly of a large number of such devices on a

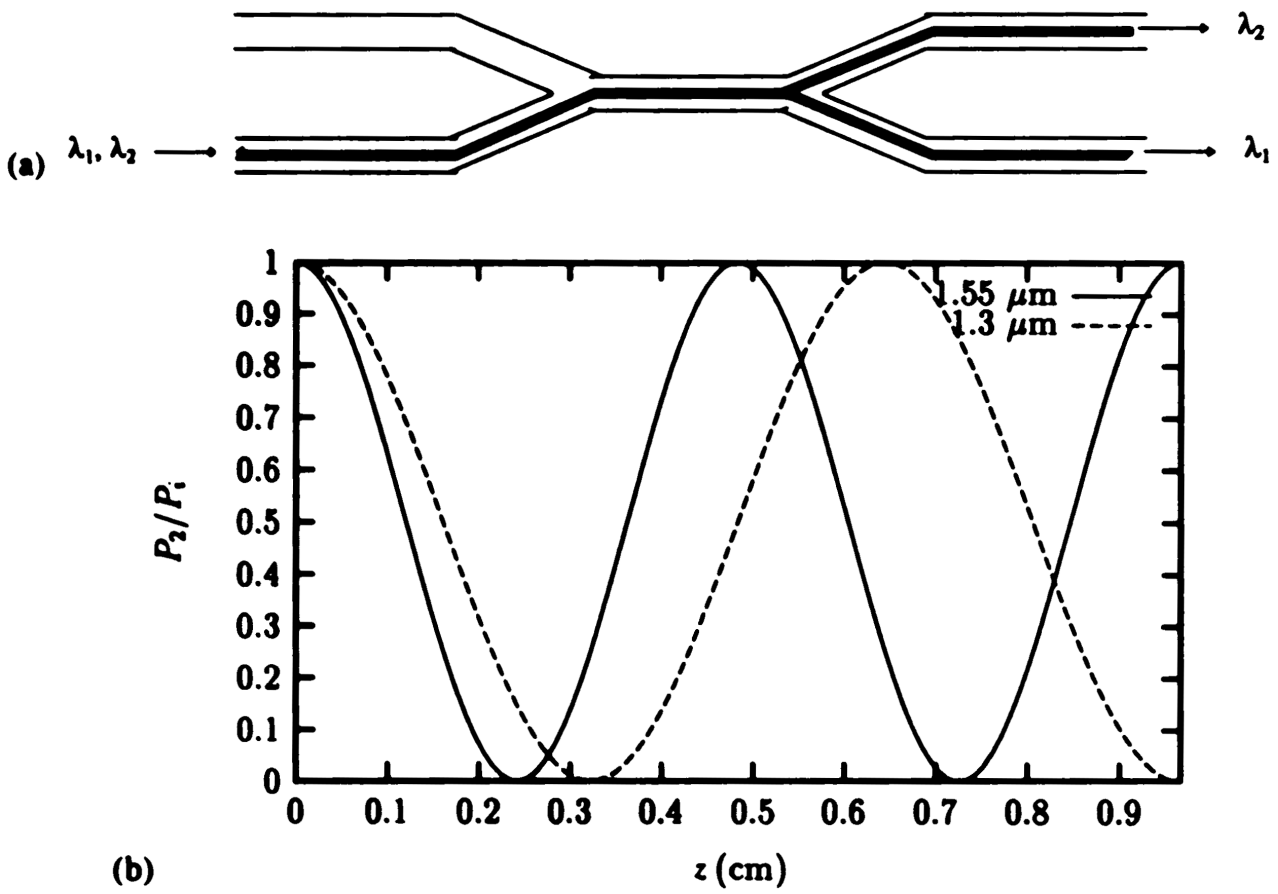

Figure 8.14 (a) A directional coupler as a wavelength division demultiplexer. The length L is chosen so that for wavelengths λ_1 and λ_2, the equations referred to in the text are satisfied. In such a case, light of wavelength λ_1 exits from the input fibre, whereas that of wavelength λ_2 exits from the coupled fibre. (b) The corresponding calculated variation of the normalised power exiting from the second fibre with z for a fibre coupler made with fibres characterised by $n_1 = 1.4525$, $n_2 = 1.45$ and $a = 5.6$ μm.

single substrate. Most device elements are currently based on single mode planar optical waveguides.

The original concept of IO was proposed by Anderson in 1965 and considerable progress has been made since then. After initial research into the devices themselves, current work focuses on the problem of device integration. One of the main difficulties has been that no one substrate is ideally suited for all the different types of device.

2.2 Asymmetrical waveguides

Generally, waveguides used in IO systems are asymmetrical. Figure 8.15 shows a typical structure. The layers above and below the guiding layer have different refractive indices. the topmost layer (of refractive index n_0) is often air and consequently has a much lower refractive index than either the guide layer (n_1) or the substrate (n_2); such a guide is thus referred to as a *strongly* asymmetric guide. Unlike the symmetric case, it turns out that there is a minimum thickness below which it is not possible for the guide to support a single mode. The condition that only a single mode propagates is given by

$$\pi \leq \frac{4\pi n_1 d \cos\theta_{c2}}{\lambda_0} \leq 3\pi$$

where d is the thickness of the layer and θ_{c2} is the critical angle at the lower face. For $LiNbO_3$, this requirement becomes

$$1.51 \leq d/\lambda_0 \leq 6.02.$$

The exact value chosen for d/λ_0 depends on the manufacturing process. It is usually desirable that the guide be as thick as possible and a suitable design thickness is $d \sim 5\lambda_0$.

The field distribution can be derived in a manner similar to that used for a symmetric guide, and is illustrated for a TE_0-type mode in figure 8.16. Note the peak is displaced towards the n_2/n_1 interface, and that the mode decays more rapidly on the air side.

The above analysis assumed an infinitely wide waveguide. In practice, most waveguides used in IO have an approximately rectangular cross-section so that there is confinement in both the x and y directions. Some typical waveguide configurations are illustrated in figure 8.17. A full solution for these guides is complex, but in general it is found that in single mode guides the dimensions in both the x and y directions should be of the order of a few times the propagating wavelength, and that the mode fields should peak within

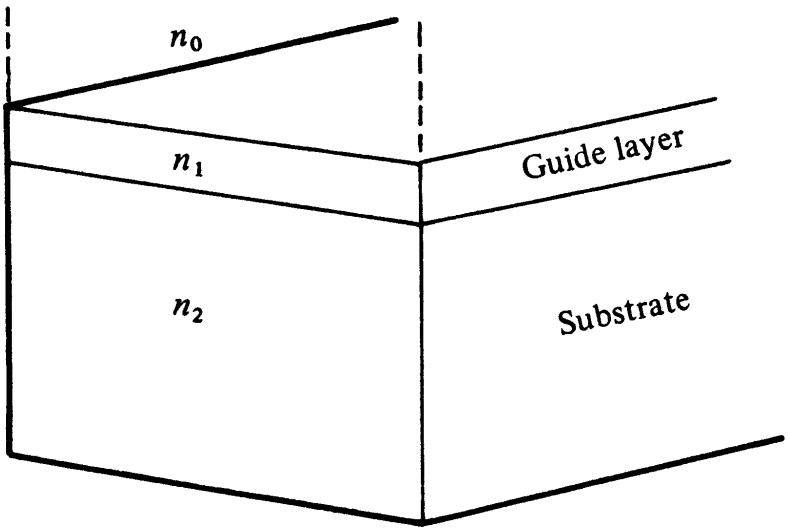

Figure 8.15 Slab planar waveguide. The guide itself is formed on a substrate. The medium above the guide is usually air. The refractive indices of substrate, guide and topmost layer are n_2, n_1 and n_0.

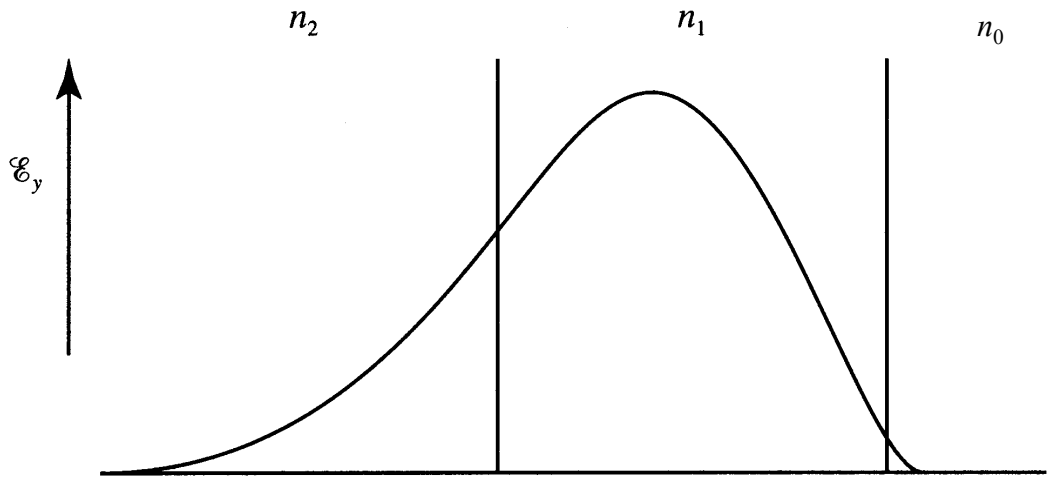

Figure 8.16 The TE_0 field distribution within a strongly asymmetric planar waveguide, where $n_1 - n_0 >> n_1 - n_2$.

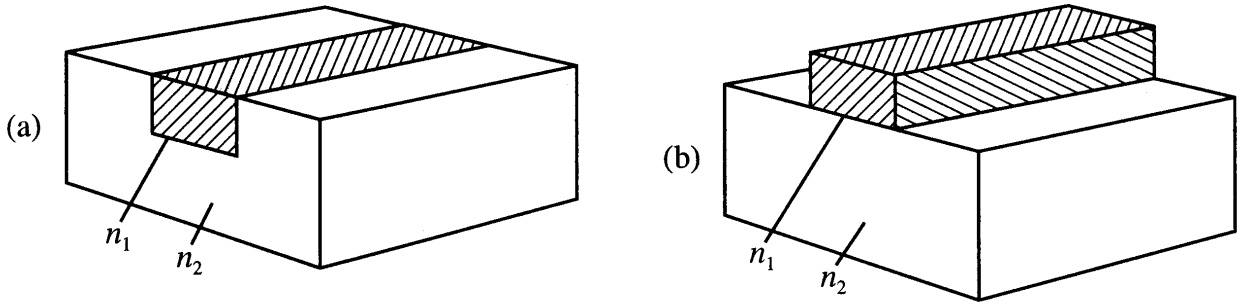

Figure 8.17 Two basic geometries used for making IO stripe waveguides: (a) the channel waveguide; (b) the ridge waveguide.

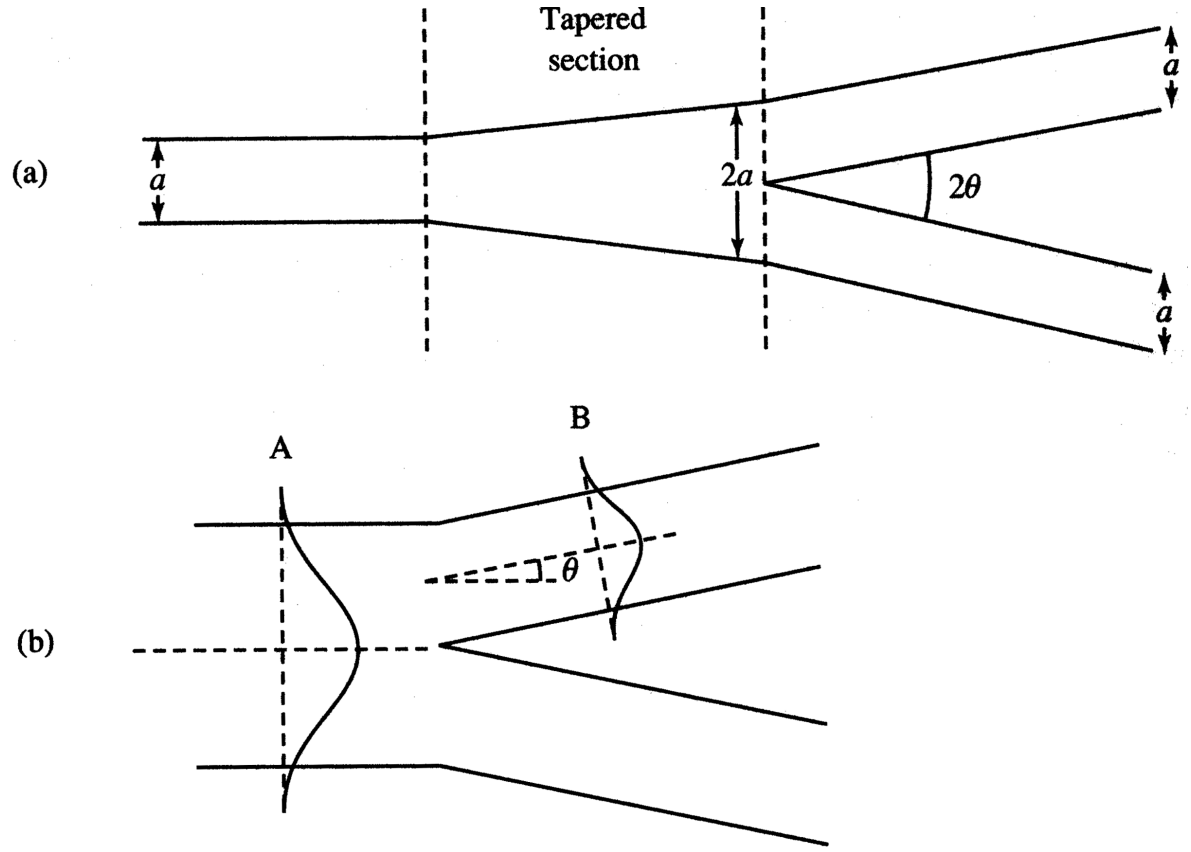

Figure 8.18 (a) A waveguide `Y' branch with an angle 2θ between the guides. (b) The efficiency of the splitting process as a function of θ can be calculated by determining the overlap integral of the waveguide modes at points just before (A) and just after (B) the branch point.

the core of the guide. Popular materials for the manufacture of these guides include materials with high electro-optic coefficients such as lithium niobate and semiconductor materials such as GaAs and GaAlAs. Losses in IO waveguides are usually much higher than in optical fibres, being $\sim 0.1\,\mathrm{dB\,mm^{-1}}$. One reason for this is the large scattering at the upper surface, which is often relatively rough. Another problem is that bends with radii less than $\sim 1\,\mathrm{mm}$ have to be avoided, otherwise losses would get too large.

2.3 Basic IO structural elements

Just as in the fibre directional couplers discussed above, one of the simplest waveguide devices is a splitter. This is illustrated in figure 8.18. In the first section of this device the waveguide expands gradually to twice its original width a and then the guide splits into two sections each of width a and angled at θ to the original direction. Energy that is in the original section of the guide will divide itself equally between the two output guides. To avoid high losses the angle between the two output waveguides ($= 2\theta$) must be small (usually less than one degree).

One of the simplest *active* devices is a phase modulator, which is similar to a Pockels cell. A stripe waveguide is formed within a suitable optically active material such as $LiNbO_3$ and electrodes are formed on the substrate surface on either side if the guide as shown in figure 8.19. If the electrodes are a distance D apart and extend for a length L, then the additional phase shift $\Delta\phi$ produced when a voltage V is applied across the electrodes is,

$$\Delta\phi = \frac{\pi}{\lambda_0} r n_1^3 V \frac{L}{D}$$

where r is the guide material electro-optic coefficient. A big advantage over bulk Pockels effect devices is that the ratio L/D may be made relatively large (~ 1000) and a phase change of π may then be achieved with voltages as low as 1 V or so.

A high-speed switch/modulator may be made by incorporating the phase shifter into one arm of the interferometer arrangement shown in figure 8.20. This configuration is known as a *Mach–Zehnder* interferometer. In it the guide splits into two with both paths rejoining after an identical path length. With no applied voltage across the phase shifter, the radiation in the two arms will have the same phase when they recombine, and hence the device will not affect the radiation flowing along the guide. However, if the phase shifter is activated to give a phase shift of π, then, on recombining, the radiation in the two arems will interfere destructively and no radiation will proceed down the guide.

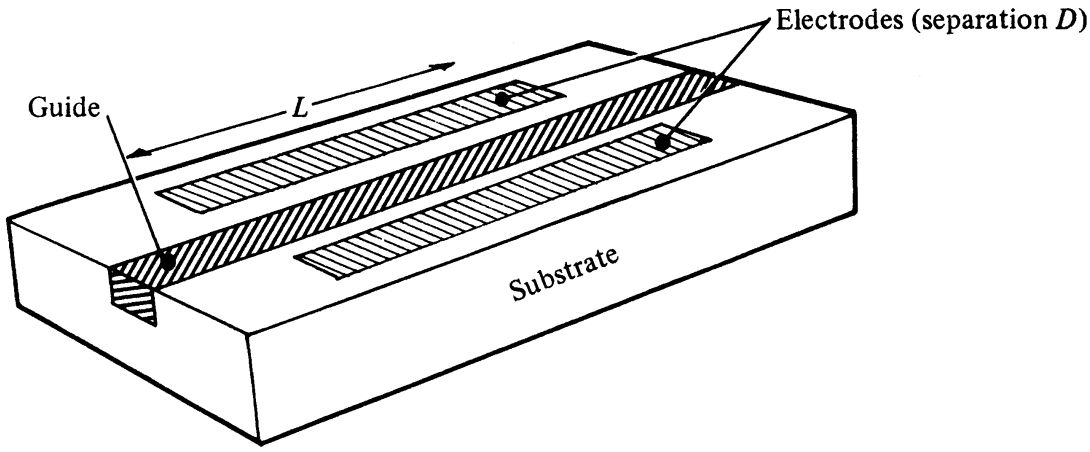

Figure 8.19 Integrated optical version of the Pockels cell that can be used as a phase shifter.

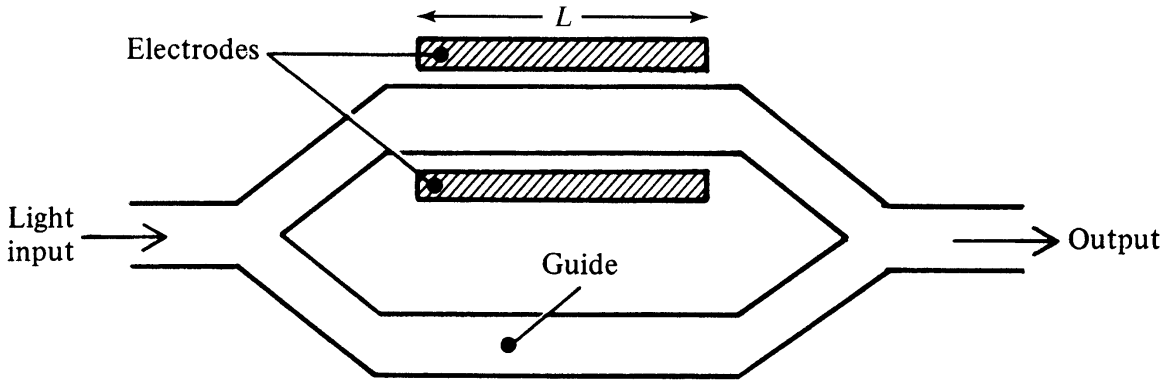

Figure 8.20 Interferometric modulator; a voltage applied across the electrodes affects the refractive index of the upper guide over a distance L.

Commercial $LiNbO_3$ devices have modulation capabilities of up to a few tens of gigahertz.

As in the case of fibres discussed above, it is also possible to build a directional coupler using waveguide technology, and indeed the transmission properties of such guides are illustrated in figures 8.6 and 8.7. It is possible to control the coupling, and several configurations have been developed to implement this. One such is shown in figure 8.21. Electrodes are deposited above each waveguide and a potential is applied between them. The opposing vertical fields in the two waveguides can, if the material axes have been chosen correctly, induce opposite changes in the guide refractive indices, and hence change the value of $\Delta\beta/2\kappa$.

Devices such as filters and resonators can be realized in IO by incorporating periodic structures into optical waveguides. Consider, for example, a waveguide with a 'corrugation' etched upon its surface perpendicular to the direction of beam propagation (figure 8.22). This structure is encountered in the distributed feedback laser discussed by Dr. Baird; it acts as a wavelength-dependent mirror, *i.e.* strong reflection occurs when $2D = m\lambda_0/n_1$, where D is the grating period, λ_0 the vacuum wavelength, n_1 the guide material refractive index and m an integer. Reflection bandwidths are usually narrow, but may be increased by 'chirping' the grating (figure 8.23).

It is also possible to construct devices based on slab waveguides. For example, a beam deflector is based on diffraction from an acoustic wave. An interdigital electrode structure deposited on a suitable acousto-optic material (figure 8.24) can generate a beam of surface acoustic waves which can then serve to diffract light travelling along the guide. The angle through which the beam is diffracted may be changed by varying the frequency (and hence the wavelength) of the acoustic wave.

When it comes to emitters and detectors the most obvious choice for a substrate would seem to be a semiconductor. Since most of the devices above are based on materials with a large electro-optic coefficient such as $LiNbO_3$, it is obvious that the optimum substrate materials for modulators and emitters/detectors do not necessarily coincide. Semiconductor lasers absorb light when no current is present. Thus it is necessary in a semiconducting IO device to couple the light from the semiconductor laser into a semiconducting waveguide beneath. This is illustrated in figure 8.25. Modern IO systems based on semiconductors make extensive use of multiple quantum well devices, and I will discuss some of these in lecture 10.

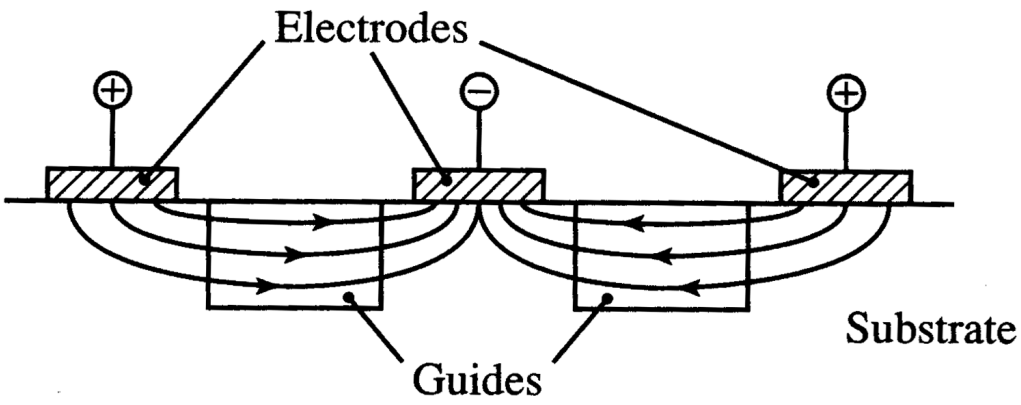

Figure 8.21 An electrode configuration used to modify the propagation conditions in two adjacent waveguides in order to alter the coupling of radiation between them. The electric fields are in opposite directions through the guides and hence the effective refractive index of one guide will be raised whilst that of the other will be lowered.

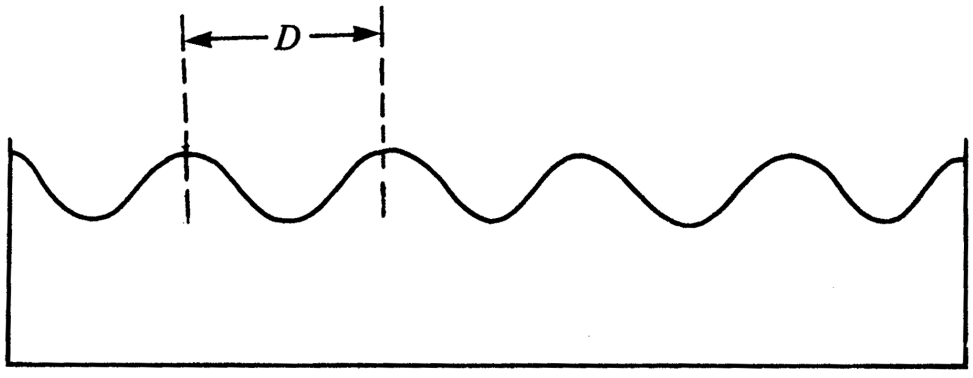

Figure 8.22 Waveguide with a corrugation of period D etched upon it.

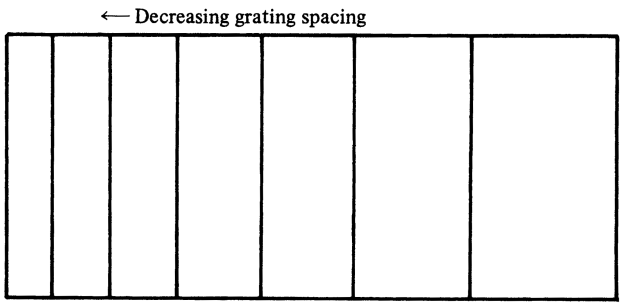

Figure 8.23 `Chirped' diffraction grating structure. The lines represent the grating peaks.

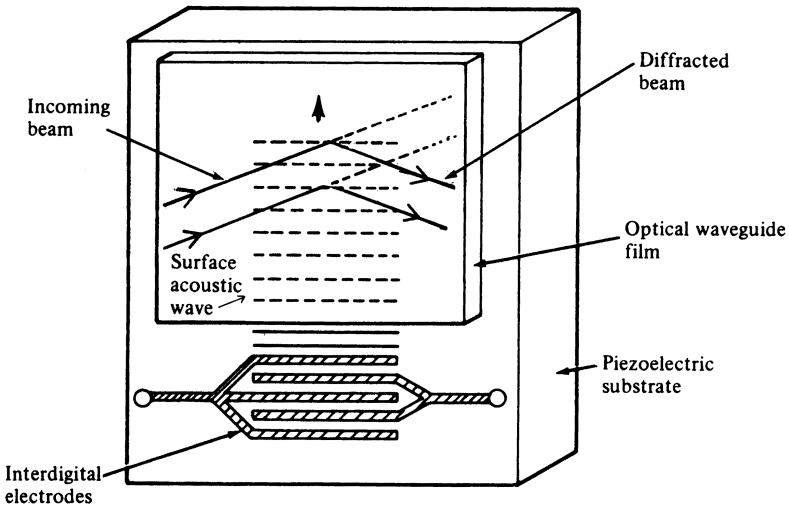

Figure 8.24 Beam deflection using diffraction from a surface acoustic wave generated by applying an alternating voltage to an interdigital structure evaporated onto the surface of a piezoelectric substrate.

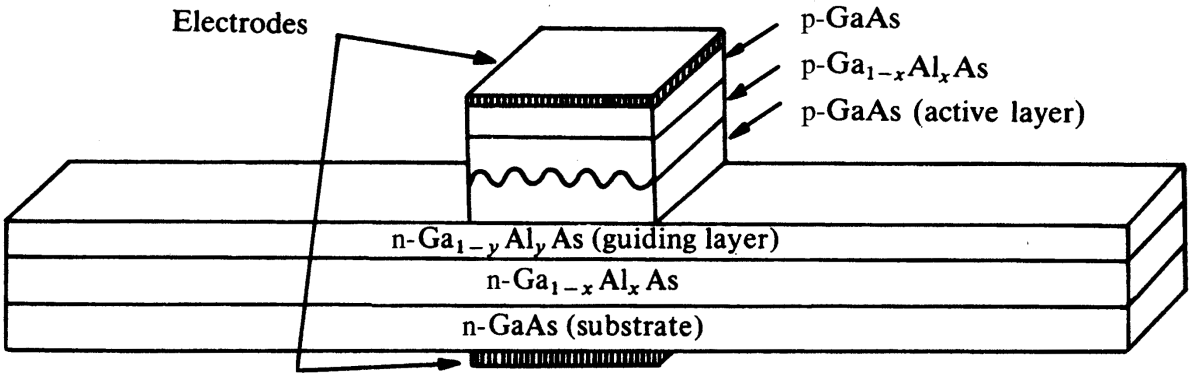

Figure 8.25 IO semiconductor laser based on GaAs/GaAlAs using Bragg reflectors instead of cleaved end mirrors. Light from the active layer is coupled into the layer beneath, which then acts as a waveguide.

2.4 IO devices

An early IO device was an optical spectrum analyser, designed to display the frequency spectrum of a radio-frequency (RF) signal. The layout is shown in figure 8.26. Light from a semiconductor laser is launched into a waveguide and the beam subsequently rendered parallel by the use of a 'geodesic' lens. This is a circular indentation made in the substrate layer with the guide layer thickness being unchanged across the indentation. Such a structure behaves like a 'one-dimensional' lens. The parallel beam then passes through the acousto-optic beam deflector. If a single RF frequency is present, the amount of deflection will depend upon the instantaneous value of the frequency. A second lens subsequently focuses the light onto a particular photodetector in a photodiode array. Each detector element thus corresponds to a narrow range of RF frequencies, and the device functions as an RF spectrum analyser. This is not a pure IO device, as the emitter and detector are separate components.

Figure 8.27 illustrates an integrated laser emitter–external modulator combination for use at $1.55\,\mu$m which has been demonstrated by AT&T Laboratories. The laser, modulator and connecting waveguide are based on quantum well structures and the laser has and external Bragg reflector for feedback. Within the laser itself the eight quantum wells are based on compressively strained layers of InGaAs/InGaAsP, whereas within the modulator there are 10 layers based on InGaAsP/InP. The whole is based on an InP substrate. Other examples of communication-oriented IO devices that have been successfully demonstrated are a balance heterodyne receiver and a tunable transmitter for wavelength division multiplexing.

3 Soliton Fibre Communications

3.1 Introduction

As Dr. Baird discussed in one of his lectures, when non-linear effects such as self-phase modulation (SPM) are taken into account, then around $1.55\,\mu$m, where the group velocity dispersion (GVD) becomes negative, solutions exist for the propagation of pulses along a fibre known as SOLITONS. The pulse stretching due to SPM is compensated for by the GVD, and the pulse shape remains stable along the fibre, provided the intensity is kept within certain limits. In fact, optical solitons in fibres constitute a whole family of pulses with different peak powers for a given pulse width. The members of the family are

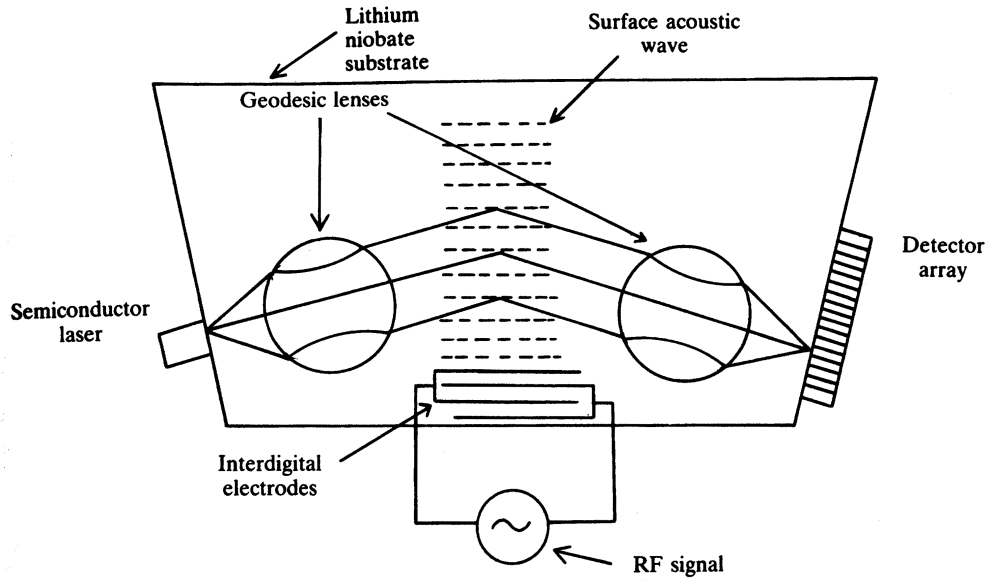

Figure 8.26 Integrated optical spectrum analyser based on an acousto-optic deflector.

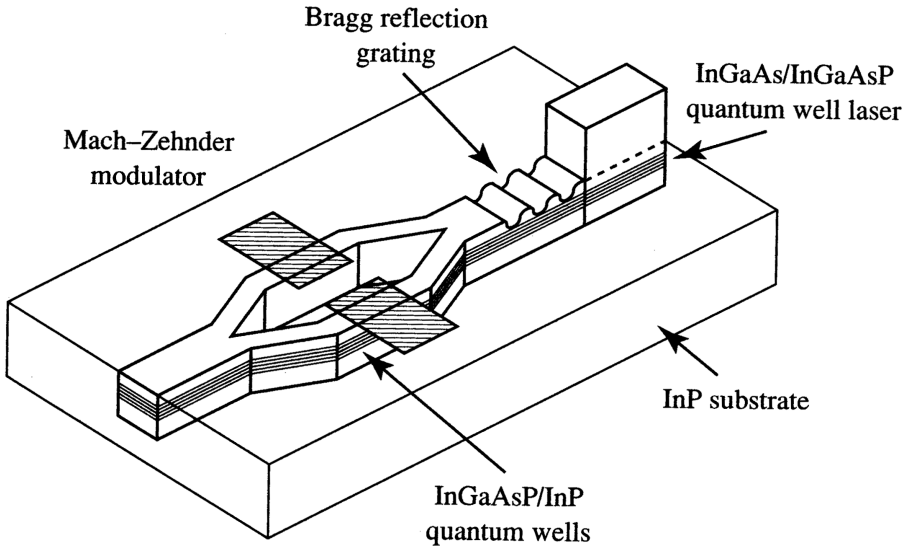

Figure 8.27 An integrated optical emitter-modulator combination based on a quantum well semiconductor laser and a Mach-Zehnder-type modulator.

characterized by a parameter N, called the order of the soliton. The Nth-order soliton has the peak power $P_N = N^2 P_s$, where P_s is the peak power of the first-order (called fundamental) soliton and N is a positive integer. These solitons are in fact solutions of the non-linear Schrödinger equation which governs the propagation of intense light pulses along fibres, and are the "bound" states of this equation. An input pulse propagating in the fibre can excite one or more of these non-linear bound states together with a continuum of states which correspond to linear dispersive waves. If the input pulse shape, width and power are such that they correspond closely to a specific bound state, no dispersive waves will be generated, and the pulse will propagate as a soliton whose order is determined by the input-pulse peak power. Figure 8.28 (a) - (c) shows the evolution of first-, second- and third-order solitons, respectively. In all cases, solitons recover their shape after propagating over a distance known as the soliton period, $\xi_s = \pi/2$. The first-order soliton has the property that neither its shape nor its phase (figure 8.25 (d)) changes during propagation.

3.2 Stability of solitons in real systems

Because of their particle-like nature, solitons remain stable under most perturbations (such as chirp, fibre loss and amplifier noise). As an example of soliton robustness, the peak power necessary to generate a fundamental soliton lies in a range as broad as $0.25P_s < P_{in} < 2.25P_s$. Within this range of peak power, an input pulse will become a fundamental soliton after propagating over a few dispersion lengths.

Long-distance transmission of information using optical fibres is (as I've mentioned many times in this course) hampered by three main types of signal degradation, which are intrinsic to the fibre — loss, dispersion and non-linearity. Fibre loss can be minimised by operating near $\lambda = 1.55\,\mu$m. However, even with fibre loss as low as $0.2\,$dB/km, the signal power is reduced by 20 dB (a factor of 100) after transmission over 100 km of fibre. The loss problem can be solved by periodically using in-line optical amplifiers to restore the signal power to its original level. Fibre dispersion then becomes the most limiting factor for long-haul systems. The use of a dispersion-compensated scheme can solve the problem to some extent, but the system performance is then limited by the fibre non-linearity. Solitons provide an ideal solution to this problem since they use fibre dispersion and non-linearity to their advantage in such a way that the two "harmful" effects become useful. This is the main reason behind the enormous interest in soliton communication

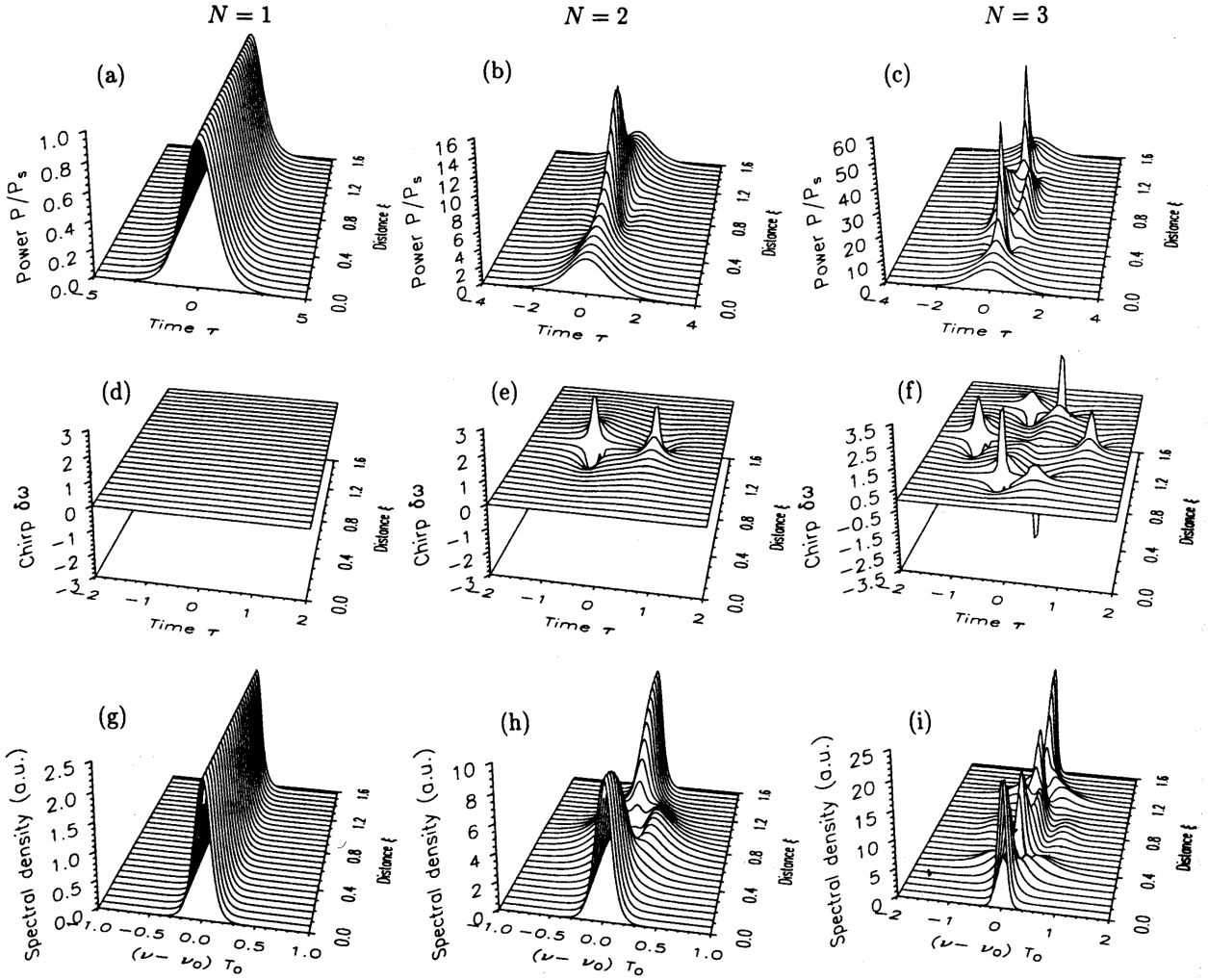

Figure 8.28 Temporal, chirp and spectral evolution of $N = 1$, $N = 2$ and $N = 3$ solitons over one soliton period. Although all solitons periodically recover their shape only the fundamental soliton preserves its shape and does not develop chirp during propagation.

systems.

3.3 Practical realisation

The first experiment that demonstrated the possibility of soliton transmission over transoceanic distances was performed in 1988 by Mollenauer and Smith. They used a recirculating fibre loop whose loss was compensated through a Raman amplification scheme. The experiment used large pulsed laser systems, and it was the availability of EDFAs by the end of 1989 which enabled the amplification of picosecond pulses emitted by semiconductor lasers, enabling sufficient peak power to allow fundamental solitons to be maintained in the fibre. By 1990 many groups worldwide were busy demonstating soliton based communication systems. Systems operating at 20Gb/s for a single channel over distances in excess of 10 000 km have been demonstrated. The next transpacific cable (TPC-6) will make use of soliton-like propagation. It began to be planned in 1996 and is due for completion in 2000. The pulse widths used are ~ 20 ps. Existing fibres have too great a dispersion at 1.55 μm to take a higher bit rate. Newer fibres have been demonstrated with pulse widths od 3 ps and a bit rate of 100 Gb/s. These systems are still under development, however.